

Validation of Smart Nanoparticles as Controlled Drug Delivery Systems: Loading and pH-Dependent Release of Pilocarpine

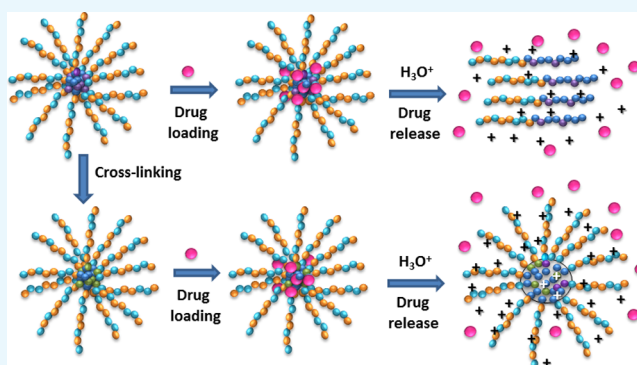
Elsa Galbis,[†] Nieves Iglesias,[†] Ricardo Lucas,[†] Ernesto Tinajero-Díaz,[‡] M.-Violante de-Paz,^{*,†} Sebastián Muñoz-Guerra,[‡] and Juan A. Galbis[†]

[†]Departamento de Química Orgánica y Farmacéutica, Facultad de Farmacia, Universidad de Sevilla, 41012 Sevilla, Spain

[‡]Departamento de Ingeniería Química, Escuela Técnica Superior de Ingenieros Industriales de Barcelona, Universidad Politécnica de Cataluña, 08028 Barcelona, Spain

Supporting Information

ABSTRACT: Micelles are good devices for use as controlled drug delivery systems because they exhibit the ability to protect the encapsulated substance from the routes of degradation until they reach the site of action. The present work assesses loading kinetics of a hydrophobic drug, pilocarpine, in polymeric micellar nanoparticles (NPs) and its pH-dependent release in hydrophilic environments. The trigger pH stimulus, pH 5.5, was the value encountered in damaged tissues in solid tumors. The new nanoparticles were prepared from an amphiphilic block copolymer, [(HEMA_{19%}-DMA_{31%})-(FMA_{5%}-DEA_{45%})]. For the present research, three systems were validated, two of them with cross-linked cores and the other without chemical stabilization. A comparison of their loading kinetics and release profiles is discussed, with the support of additional data obtained by scanning electron microscopy and dynamic light scattering. The drug was loaded into the NPs within the first minutes; the load was dependent on the degree of cross-linking. All of the systems experienced a boost in drug release at acidic pH, ranging from 50 to 80% within the first 48 h. NPs with the highest degree (20%) of core cross-linking delivered the highest percentage of drug at fixed times. The studied systems exhibited fine-tuned sustained release features, which may provide a continuous delivery of the drug at specific acidic locations, thereby diminishing side effects and increasing therapeutic rates. Hence, the studied NPs proved to behave as smart controlled drug delivery systems capable of responding to changes in pH.



INTRODUCTION

The use and development of micro/nanostructures in smart drug/gene delivery systems have caught the attention of the research community for the last two decades or so, and some interesting reviews have summarized the last trends in this field.^{1–3} The controlled drug delivery is not only advantageous in suppressing the side effects of the toxic drugs but also in overcoming the drawbacks of insoluble drugs, especially of anticancer molecules such as doxorubicin.⁴ Among the most promising systems, organic nanoparticles (NPs) are being widely studied. The formation of organic nanoparticles can be achieved not only by the self-assembly of two mixed components of opposed hydrophilic/hydrophobic nature⁵ but also by the use of amphiphilic block copolymers, leading to nanosized micelles.⁶ By ensuring the homogeneity of the generated nanoparticles, the latter method allows the reliable preparation of formulations widely used in varied fields, from drug delivery, biosensors, and gene therapy to cosmetics, among others.^{2,7}

In the face of common drawbacks in therapeutic treatments, such as the difficulty of getting the drug across biological barriers and reaching the damaged tissue or the degradation

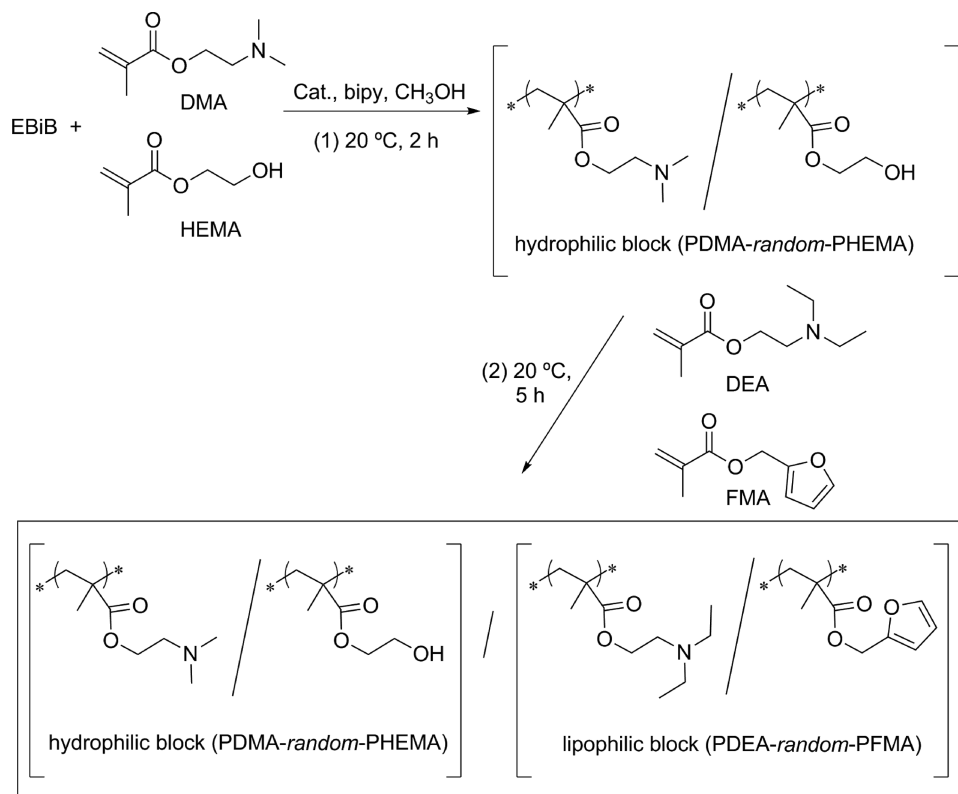
that takes place once the drug enters the organism, smart nanosized systems have become the option of choice. The internal hydrophobic nature of the NPs would protect the drug against the degradative environment on its way to the biological target.

Micelles from diblock copolymers are one of the most popular drug delivery systems (DDS), leading to core-shell micelles, which are able to transport lipophilic molecules into its core.^{1,8} ABC triblock copolymers are another option which leads to the formation of core-shell-corona micelles. The presence of a highly hydrophilic corona layer makes them very stable in aqueous media.^{4,9} Methacrylate esters,¹⁰ poly(ethylene glycol),^{4,11} and chitosan¹² among others are the most common hydrophilic segments, and regarding the hydrophobic blocks, polycaprolactone,⁴ poly(propylene oxide),¹³ poly(dimethylsiloxane),¹⁰ cyclodextrins,^{2,11} and other methacrylate derivatives¹⁴ can be found.

Received: September 25, 2017

Accepted: December 25, 2017

Published: January 11, 2018

Scheme 1. One-Pot Synthesis of Methacrylate-Based Block Copolymers by ATRP^a

^aInitiator: ethyl-2-bromo-2-methylpropionate (EBiB); catalyst: CuBr; ligand: 2,2'-bipyridyl (bipy).

Moreover, the so called smart NPs can be designed in such a way that they respond to changes within the human body as a means of boosting the drug concentration where it is required. One highly useful trigger stimulus is the reduction in pH commonly encountered in cancerous tissues of solid tumors. The presence of tertiary amine groups in the block copolymers imparts pH-responsive properties to the final micelles, as has recently been confirmed.¹⁵ However, the dynamic, reversible nature of micelle formation is a source of instability. As the micelles can be dissociated at low concentrations (below its critical micelle concentration), the premature drug release at normal tissues or organs may be accelerated, prompting serious side effects.⁴ The disruption of NPs by dilution can be prevented if they are properly cross-linked, either in the shell, or in the core,¹⁶ leading to stable unimolecular NPs, the former option being the most widely investigated. The core cross-linking approach circumvents the potential intermicellar reaction because the hydrophilic block in the shell acts by minimizing the chain overlap between adjacent micelles via a steric stabilization mechanism, thus preventing intermicellar cross-linking.¹⁷

Our research group has carried out the preparation of smart, pH-responsive core cross-linked NPs as potential DDS,¹⁵ and the aim of the present work is the validation of these NP dispersions as drug carriers able to control the release of an active lipophilic molecule upon a trigger stimulus. As far as the authors are aware, this is the first time that the influence of the degree of core cross-linking in the uptake and release of a hydrophobic drug has been investigated in NPs used as DDS. Pilocarpine, a hydrophobic drug, was the molecule of choice. The uptake kinetics of the drug by cross-linked and non-cross-linked systems were compared, as well as its release under

various conditions. The findings were supported by data collected from scanning electronic microscopy (SEM), dynamic light scattering (DLS), UV-visible spectroscopy, and other techniques.

RESULTS AND DISCUSSION

Preparation of NPs from the Autoassembly Block Copolymer [(DMA_{31%} HEMA_{19%})-*block*-(DEA_{45%}-FMA_{5%})] (Samples S1, S2, and S3). The preparation of the amphiphilic block copolymer used in the present work has been published elsewhere¹⁵ and is summarized in Scheme 1. The synthesis was carried out by the widely used atom transfer radical polymerization (ATRP) at ambient temperature, a “living” polymerization procedure that allows the reliable formation of block copolymers by means of one-pot reactions. In this case, the hydrophilic block, constituted by *N,N*-dimethylaminoethyl methacrylate (DMA) and 2-hydroxyethyl methacrylate (HEMA) monomers, was formed first, followed by the subsequent addition of the hydrophobic monomers *N,N*-diethylaminoethyl methacrylate (DEA) and furfuryl methacrylate (FMA), leading to the formation of the hydrophobic block. The experimental copolymer composition (in mole percentage), determined by proton nuclear magnetic resonance (¹H NMR), was found to be [(DMA_{31%} HEMA_{19%})-*block*-(DEA_{45%}-FMA_{5%})]. The values of molecular weights and polydispersity were calculated by gel permeation chromatography and were found to be $M_n = 34\,700$; $M_w = 45\,100$; and $M_w/M_n = 1.3$.

The autoassembly features of that copolymer in aqueous media were studied. The properties of the generated NPs, such as size, polydispersity, shape, and critical micelle concentration (CMC),^{18,19} were explored by means of various techniques:

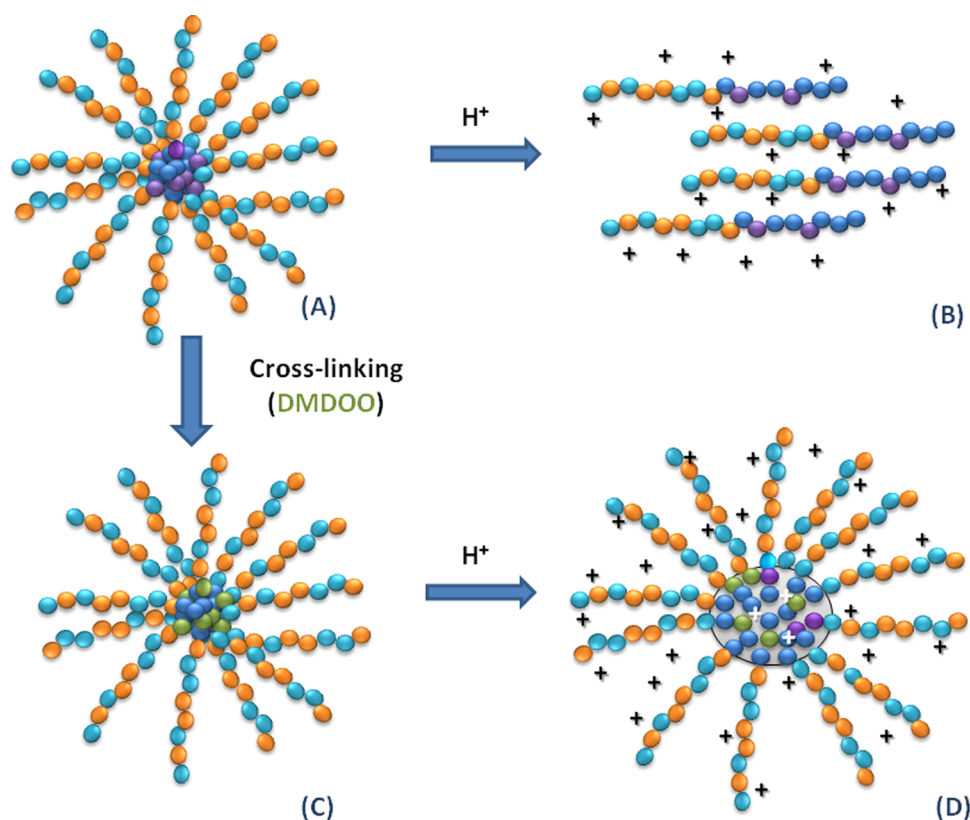


Figure 1. (A) Micelles from autoassembly of the amine-containing amphiphilic block copolymers in aqueous media (nonstabilized micelles); (B) solution of protonated polymer chains, (C) stabilized NPs by core cross-linking; and (D) stable amine-containing NPs with hydrophilic and hydrated core.

SEM, DLS, UV–vis spectroscopy, and others. The CMC value (0.078 mg/mL) demonstrates the great tendency to self-assemble into micelles in aqueous media. Accordingly, well-defined micelles were formed at pH 7.0 (Figure 1A) when the polymer concentration stood at 0.25 mg/mL (sample S1). The hydrophobic blocks, formed by DEA/FMA moieties, constituted the dehydrated micelle cores,¹⁷ leaving the hydrophilic blocks (formed by DMA and HEMA moieties) in the outer part of the NPs in contact with the aqueous medium.

The disruption of these micelles can be a priori boosted by dilution or under acidic environment (Figure 1B). The use of a cross-linker can lead to the formation of covalent bonds between the furan moieties present in the core (Figure 1C). Thus, the micellization would become irreversible once the cross-linking reaction took place, making them stable under those conditions, whether at high dilution or at acid pH (Figure 1D). Consequently, another two systems were prepared at the same polymer concentration, with the aim of core cross-linking the micelles and hence obtaining stable NP dispersions. To accomplish this requires a simple, fast, and reliable reaction with some specific features (e.g., high yields and absence of side products). Those reactions that meet such attributes are grouped under the denomination of click reactions, the Diels–Alder reaction being one of them. One of the most widely used Diels–Alder reactions is that involving a maleimide ring and a furan ring.²⁰ Thus, furan rings present in the micellar core would react in pairs with the two maleimide groups from the freshly prepared cross-linker (1,8-dimaleimide-3,6-dioxaoctane, DMDOO). The degree of cross-linking was fixed in these assays (sample S2 with 20% of cross-linking, and sample S3

with 10% of cross-linking) so that two dispersions of stable NPs were achieved (Figure 1C).

Size and Shape Morphology of NPs S1–S3 and Stability at pH 5.5 (ac-S1 to ac-S3). The shape and surface morphology of prepared NPs were evaluated by SEM and DLS. The studies revealed that most of the NPs were fairly spherical in shape. Studies carried out on S1 demonstrated the formation of dispersions with a low polydispersity index (PDI, 0.14) and average hydrodynamic diameter (D_h) by DLS of 210 nm (Table 1). As far as the dispersions S2 and S3 are concerned, the cross-linking of the NPs resulted in a minor increase in PDI in both assays (to values close to 0.3), with the main population of NPs (95% of the total) at just over 100 nm (Table 1). The analyses of SEM images revealed, first, that the average particle sizes of samples S1, S2, and S3 were 95, 49, and 65 nm, respectively, which evidenced an overestimation of NPs' sizes by DLS. On the other hand, a significant reduction in size (between 31 and 48% from SEM data) was observed for the cross-linked NPs, in comparison with sample S1.

The pH of the media and the drug loading displayed a marked impact on the NP size. At acidic pH, not only did the cross-linked NPs (ac-S2 and ac-S3) undergo a dramatic increase in size (from 5 to 10 times) but this effect was also dependent on the degree of cross-linking. The same trend was also encountered when loading NPs were analyzed (LS1, LS2, and LS3). This observation is well depicted in Figures 2 and 3 and discussed below.

The success of the stabilization process was investigated by both dilution and treatment at acidic pH. When dispersions were diluted with dimethylformamide to concentrations below CMC, the only samples that remained stable were those with

Table 1. Comparison of Z-Average, Polydispersity Index (Pdl), Hydrodynamic Diameter (D_h), and Zeta Potential (ζ)^a

degree of cross-linking	pH = 7.0 (unloaded) ¹⁵					pH = 5.5 (unloaded)					pH = 7.0 (loaded)				
	sample	Z-average (\pm SD) (nm)	Pdl (\pm SD)	size (\pm SD) (D_h , nm)	ζ (\pm SD) (mV)	sample	Z-average (\pm SD) (nm)	Pdl (\pm SD)	size (\pm SD) (D_h , nm)	ζ (\pm SD) (mV)	sample	Z-average (\pm SD) (nm)	Pdl (\pm SD)	size (\pm SD) (D_h , nm)	ζ (\pm SD) (mV)
non-XL	S1	177 (\pm 1)	0.14 (\pm 0.02)	210 (\pm 80)	+12.1 (\pm 0.4)	ac-S1	186 (\pm 3)	0.34 (\pm 0.02)	200 (\pm 100)	+45.3 (\pm 1.7)	LS1	191 (\pm 1)	0.36 (\pm 0.01)	300 (\pm 100)	+17.0 (\pm 1.7)
XL 20%	S2	108 (\pm 1)	0.33 (\pm 0.01)	130 (\pm 70)	+20.8 (\pm 0.6)	ac-S2	326 (\pm 20)	0.65 (\pm 0.02)	600 (\pm 200)	+60.7 (\pm 3.3)	LS2	440 (\pm 50)	0.52 (\pm 0.03)	380 (\pm 80)	+23.1 (\pm 3.2)
XL 10%	S3	83 (\pm 1)	0.30 (\pm 0.03)	110 (\pm 80)	+14.9 (\pm 0.1)	ac-S3	140 (\pm 1)	0.30 (\pm 0.01)	150 (\pm 70)	+55.5 (\pm 4.7)	LS3	272 (\pm 7)	0.54 (\pm 0.06)	300 (\pm 90)	+19.8 (\pm 1.8)

^aAs determined by DLS of non-cross-linked NP (non-XL) and stabilized NP at 20 or 10% of cross-linking (XL 20% and XL 10%, respectively) at pH 7.0 (unloaded or loaded with pilocarpine) and at pH 5.5.

core cross-linking (S2 and S3), validating the success of the coupling reactions.¹⁵

The samples were studied at pH 5.5 and 37 °C to reproduce the physiological conditions of pH and T to check the integrity of the NP structures in an acidic environment similar to that of damaged or targeted tissues in the human body. It was expected that the presence of DMA and DEA repeating units would make possible the protonation of both the shell and the core of the NPs. In the event that the micelles were not cross-linked, the electrostatic repulsion between the polymer chains would make them fly apart (Figure 1B). Notwithstanding, protonation in the core should not be capable of breaking the three-dimensional structure, and NPs with hydrated and hydrophilic cores could be obtained, leading to fully hydrophilic NPs (Figure 1D).

The experimental trials were conducted immersing the NPs in a buffered solution at pH 5.5 (samples ac-S1, ac-S2, and ac-S3). The findings from both DLS studies and SEM images (Table 1, Figures 2 and 3) confirmed that all of the dispersions remained stable at acidic pH, including that of the nonstabilized NPs ac-S1. Unexpectedly, and as confirmed by SEM images (Figure 2a), protonation of the polymer in sample ac-S1 was not capable of breaking up the micelles, which kept their integrity. This behavior may be due to the difficulties encountered by the acidic water solution to enter the core of the micelles and then protonate the basic residues of the DEA units, leading to a polymer solution. Besides, it is hypothesized that the high number of hydroxyl groups from HEMA moieties present in the hydrophilic blocks partially prevented the electrostatic repulsion between the cationic charges in the shell of the micelles, keeping them intact at acidic pH.

In addition, the study of the three parameters, Z-average, mean size (D_h) calculated by DLS, and mean size calculated from SEM images (Figure 3), showed that the cross-linked samples increased in size at acid pH (Table 1). The values for sample ac-S2 (with 20% of cross-linking) were significantly higher than those for sample ac-S3 (with 10% of cross-linking). Conversely, the increase in size of the non-cross-linked NPs was insignificant.

The latter findings could be explained on the grounds of the excellent packing efficiency of the polymer chains in the nucleus in nonstabilized NPs (S1/ac-S1), which would be impeded by the reaction of the bismaleimide DMDOO with the furan moieties in the nucleus of samples S2/ac-S2 and S3/ac-S3. The length of the cross-linker and the formation of two bulky tricyclic systems (Figure 4) can hinder, to some extent, the packing of the polymer hydrophobic segments in the core of the NPs. This effect is greater when the degree of cross-linking is 20%, leading to looser cores in samples ac-S2 and LS2. Consequently, the latter samples, with looser cores, enable entry of the aqueous medium into the core of the NPs. This feature had a great impact not only on the final size of the NP at pH 5.5 but also on both the loading kinetics and the percentage of drug released from each system, as described below. All in all, the dispersions S2 and S3 were stable for months, in a wide range of pH (from pH 3.0 to pH 8.0) and at high dilutions. This is supported by the study of an important colloid property, zeta potential. The samples were titrated and z-potential measured. The values were in the range from 45 to 60 mV, at acid pH, which also demonstrated the excellent stability of the prepared NPs. This remarkable stability might be attributed to the hydrophobic cross-linking cores and the steric hindrance from the hydrophilic corona. These findings

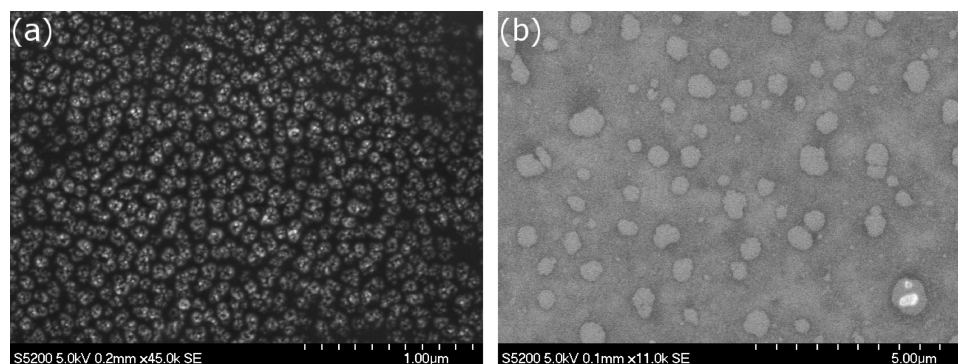


Figure 2. Selected SEM images of the NP systems at pH 5.5 prepared from the block copolymer (DMA_{31%} HEMA_{19%})-*block*-(DEA_{45%}-FMA_{5%}) synthesized by ATRP: (a) non-cross-linked NP (ac-S1); (b) core cross-linked NP with 20% of degree of cross-linking (ac-S2).

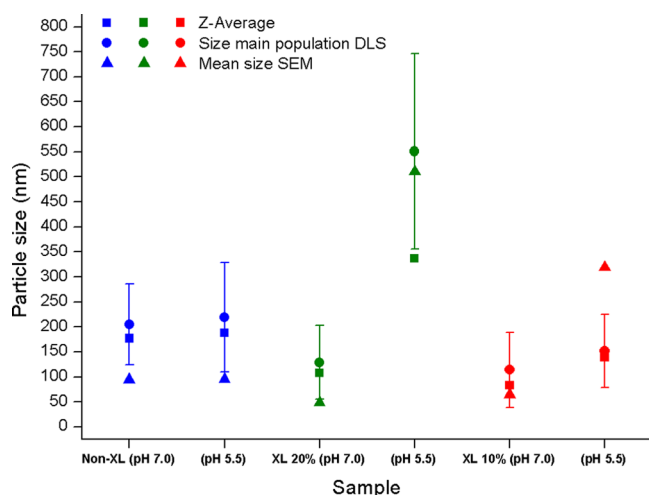


Figure 3. Comparison of mean NP sizes determined by DLS and SEM at pHs 7.0 and 5.5 (from left to right: samples S1, ac-S1, S2, ac-S2, S3, ac-S3; here “ac” denotes NPs dispersed in an acidic medium at pH 5.5, “XL” denotes cross-linked NPs and “20%” and “10%” the degree of cross-linking).

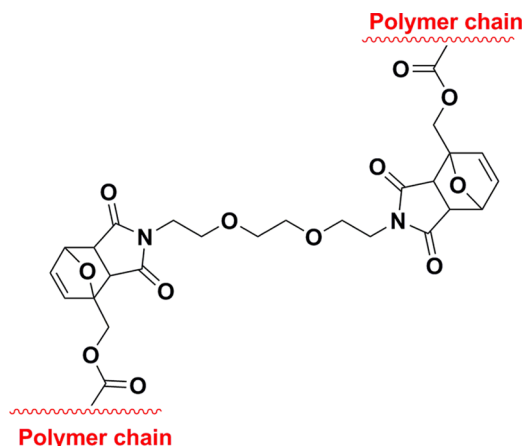


Figure 4. Diels–Alder adduct formed by the reaction of two furan rings from furfuryl methacrylate units present in the core with the cross-linker 1,8-dimaleimide-3,6-dioxaoctane (DMDOO).

support the conclusion that the prepared NPs could be promising candidates for drug delivery applications.

Loading Kinetics of Pilocarpine by the Novel Dispersions (Samples LS1–LS3). When the loading capability of the lipophilic molecules had been confirmed for

the studied NPs,¹⁵ some drug-uptake assays were carried out, using pilocarpine as the molecule of choice. Pilocarpine is a therapeutic molecule (online resource 1, Figure S1) with low water solubility and is used clinically as co-drug in glaucoma and xerostomia, as well as in the treatment of head and neck cancer; it is also prescribed against Sjögren’s syndrome. Salivary gland hypofunction, commonly developed during radiation therapy for head and neck cancer and in patients with Sjögren’s syndrome,²¹ leads to diminished secretions and the acidification of saliva. This latter characteristic would affect the regular homeostasis of the oral cavity, leading not only to specific changes in the salivary bacterial profiles²² but also to demineralization of the tooth enamel, with the consequent increase in the risk of caries.²³ In this context, because it can stimulate salivary tissues, pilocarpine is used to reduce the severity of xerostomia and salivary dysfunction. The incorporation of pilocarpine into pH-sensitive NPs allows the drug to be released under such acidic environments and exert its therapeutic activity.

Previous to the pilocarpine-loading studies, two linear regression analyses were conducted at pHs 7.0 and 5.5 to ascertain the relationship between pilocarpine concentration in aqueous solutions and its absorbance at 215 nm in UV spectroscopy (online resource 1, Figure S2). The regression analysis quantified the final concentration of pilocarpine in the media during the uptake and delivery assays.

The loading experiments were conducted at pH 7.0 and 25 °C, with a drug–polymer ratio equal to 0.8 mg of pilocarpine/mg of polymer. The drug was added, and the dispersions were analyzed at specific times. The loading of the drug by non-cross-linked and cross-linked systems was monitored for 144 h (Figure 5, assays LS1, LS2, and LS3 for non-cross-linked, 20 and 10% cross-linked NPs, respectively).

The interactions among the NPs and the drug were expected to be hydrophobic due to the chemical structure of the drug, and therefore the drug may be allocated into the core of the NP. This is supported by previous assays in which another hydrophobic and fluorescent molecule, pirenene, was embedded into NPs and was confirmed by fluorescence microscopy as well as by an extensive research carried out by other authors.^{15,24,25} The interaction of pilocarpine with the NPs at neutral pH provoked a significant drop in absorbance at 215 nm in 30 min (Figure 5A), probably due to the alteration of the excited electronic states of the drug (with impingement on the ϵ parameter). Thus, the nonloaded pilocarpine that remained in the medium may be largely responsible for the absorbance figures at 215 nm.

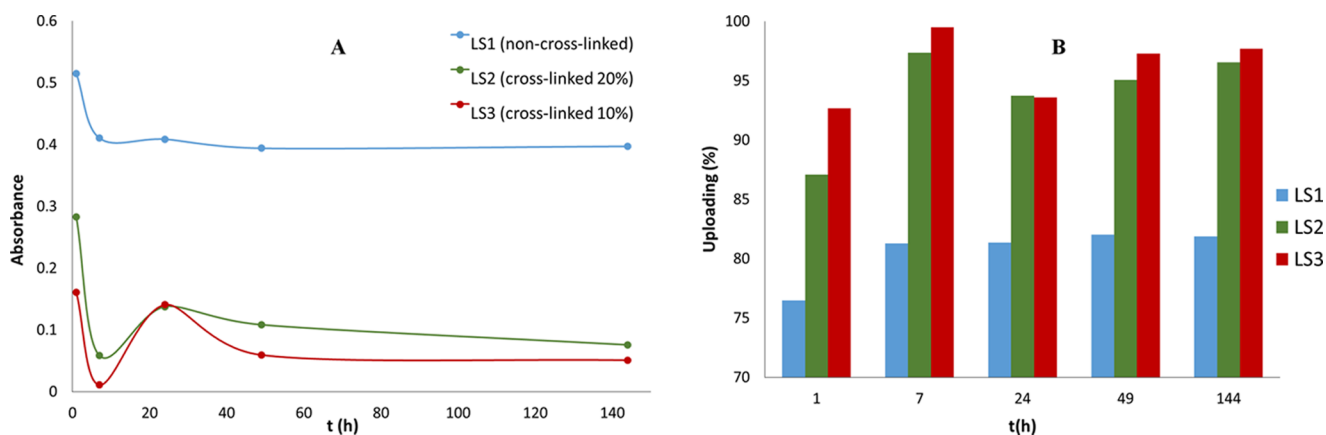


Figure 5. Kinetic studies at 25 °C of pilocarpine loading in NPs by UV–vis spectroscopy at 215 nm (initial pilocarpine concentration = 0.1 mg/mL; polymer concentration = 0.125 mg/mL). (A) Absorbance of free pilocarpine in NP dispersion vs time; (B) cumulative percentage of pilocarpine embedded into the NPs vs time, calculated from absorbance values at 215 nm.

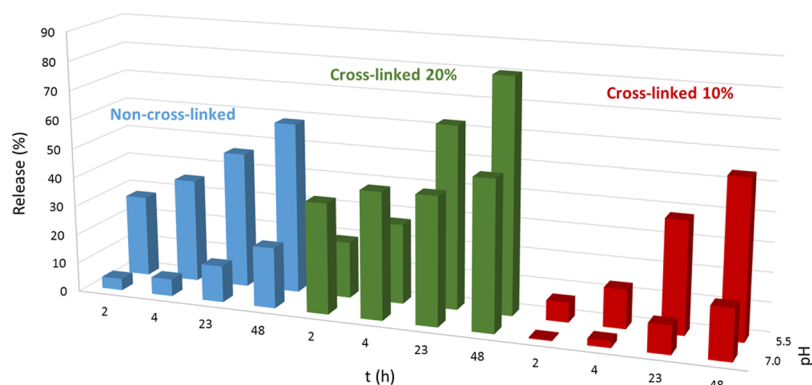


Figure 6. Release of pilocarpine (related to the entrapped pilocarpine into the NPs, in percentage) vs time from pilocarpine-loaded NPs at pHs 7.0 and 5.5 at 37 °C (polymer concentration: 0.125 mg/mL).

Therefore, the percentage of uploading was determined using the eq 1

$$\text{uploading (\%)} = \frac{\text{drug conc}_0 - \text{residual drug conc}_t}{\text{drug conc}_0} \times 100 \quad (1)$$

where uploading (%) is the entrapped pilocarpine into the NPs in percentage, drug conc₀ is the initial amount of pilocarpine at time = 0 (μg drug/mL) in the media and residual drug conc_t is the concentration of pilocarpine in the media at time = t (μg drug/mL). This last value was calculated using the eq 2, the equation being obtained experimentally from the calibration curve of pilocarpine (online resource 1, Figure S2).

$$\text{residual drug conc}_t = A/0.0227 \quad (2)$$

where A is the absorbance of the sample at 215 nm and 25 °C.

As a result, being lipophilic enough to efficiently bind pilocarpine, the NP cores removed the drug from the aqueous environment quickly. The findings also demonstrated that nonetheless the uptake is a dynamic procedure, and hence a period of stabilization of 48 h was required. This is especially important when cross-linked NPs were studied. Figure 5A displays this effect for samples LS2 and LS3. Consequently, some extra time was required to report reliable results that they were not time dependent. Conversely, once steady, the NP–drug complexes were stable for months within a wide range of temperature, from 5 to 40 °C.

Despite pilocarpine's loading efficiency being above 80% w/w in all cases (Figure 5B), a significant dissimilarity was observed between the non- and the cross-linked NPs. Thus, for example, pilocarpine was almost completely removed from the medium in LS2 and LS3 (the percentage of remaining pilocarpine was 3.5 and 2.4%, respectively), whereas just under 20% of the added pilocarpine (18%) remained in the medium without being captured by the nonstabilized NPs (LS1). Another relevant feature encountered was that the absorbance versus time curves for the uploading trials did not converge at long times, supporting the fact that those three systems behave differently as nanocarriers.

In addition, and assuming that the presence in the core of the adduct formed between the furan rings and the cross-linker DMDOO in samples LS2 and LS3 (higher ratio in the former) provides some steric hindrance and prevents the lipophilic segments of the block copolymer being tightly organized, the higher the degree of cross-linking is, the looser the cores will become. These findings demonstrated the relevance not only of the stabilization of the NPs but also of their percentage of cross-linking. On the basis of the hypothesis mentioned above, it seems that the higher the degree of cross-linking is, the higher is the free volume encountered into the core. As the drug tends to enter in the core of the NPs due to its hydrophobic nature, this could be easier once the free volume is boosted by any reason. As a result, the incorporation of the therapeutic molecule was enhanced in samples LS2 and LS3. This

conclusion is supported by size studies of loaded NPs by DLS (Table 1). In general terms, loaded NPs at pH 7.0 (samples LS1, LS2, and LS3) display higher values of Z-average and mean size (D_h) than unloaded NPs under the same conditions (samples S1, S2, and S3). The most outstanding aspects of these figures are that both Z-average and mean size markedly increased in loaded cross-linked NPs (samples LS2 and LS3), doubling and almost tripling their values compared with those of the unloaded counterparts at neutral pH. With regards to the uploading values encountered for LS2 and LS3, although being quite similar, the presence of more hydrophilic oligoethylene glycol chains of the cross-linker (Figure 4) in LS3 could diminish to some extent the affinity of the drug for the core in that sample compared to that in LS2.

Pilocarpine Release from Drug-Loaded NPs under a Trigger Stimulus (Samples RS1–RS3). The last part of the present work was focused on evaluating the release of pilocarpine from the NPs at neutral pH and in response to the acidification of the aqueous media. The acidic pH was set at 5.5 as this value corresponds to the pH encountered in oral secretions during the treatment of head and neck cancer, as well as in patients with Sjögren's syndrome. The NPs were immersed in a buffer solution (either phosphate buffer pH 7.0; or phosphate buffer pH 5.5). The drug content was evaluated by UV–vis measurements at 215 nm, using the unloaded NPs as blank. The cumulative pilocarpine release profiles from NPs at pHs 7.0 and 5.5 are shown in Figure 6.

The percent of drug release was determined using eq 3

$$\text{Drug release(\%)} = \frac{m_{\text{entrapped}(0)} - m_{\text{residual}(t)}}{m_{\text{entrapped}(0)}} \times 100 \quad (3)$$

where $m_{\text{entrapped}(0)}$ is the weight of initial entrapped pilocarpine into the NPs; $m_{\text{residual}(t)}$ is the weight of residual pilocarpine at time “ t ” into the nanocarriers.

For these trials, the use of normalized data was made to compare the capacity of the systems studied to retain or not the drug into the NPs at different pHs. At neutral pH and from the normalized values of the drug released from the NPs, some liberation was found in every case, being low for the systems RS1 and RS3, in which most of the drug remained in the NPs. These findings support the hypothesis that on one hand, the looser the core of the NP is, the easier is the diffusion of the drug to the media, this fact being more marked in the case of sample RS2, and on the other hand, the drug could be present not only in the NP core but also in the shell. Although it could be wrongly inferred from a quick view of Figure 6 that non-cross-linked NPs (RS1) are better than 10% cross-linking NPs (RS3) on releasing the drug, this was not the case.

When the loaded NPs were exposed to the trigger stimulus, i.e., the acidification of the media to pH 5.5, a boost in the drug release was observed in all systems. The protonation of the tertiary amine groups of DMA and DEA residues took place, and, as a result, the core became hydrophilic, allowing entry of the aqueous media. Consequently, the pilocarpine was no longer enclosed in a lipophilic environment and between some 50 and 80% of the drug content was released in 48 h, depending on the system. To have a better understanding of the release kinetics of the drug in the three studied systems, in the case of cross-linked NPs (RS2 and RS3), the most significant fact was that the more cross-linked the NP, the higher the observed percentage of release at fixed times. Once more, how loosely entangled the core was, played a crucial role

in the performance of the NPs as drug delivery systems. Interestingly, release figures from trials of non-cross-linked NPs (RS1) were higher than those from trials of RS3 throughout the studied period of time. It is hypothesized that some disruption of the micellar structure might have taken place, causing liberation of the drug into the media, confirming the benefits associated with the cross-linking in the NPs formed.

CONCLUSIONS

Three NP systems prepared from a new amphiphilic self-assembled block copolymer, one of them nonstabilized and the other two stabilized by means of core cross-linking, have been investigated in terms of their drug loading and release capacities under physiological conditions. The shape and structure of all of them were evaluated at pH 7.0 and pH 5.5 by scanning electron microscopy (SEM) and dynamic light scattering (DLS). At pH 7.0, NPs in the range from 100 to 200 nm with low polydispersities were found. Trials conducted in acidic media confirmed the integrity of the NP structures at pH 5.5, and an increase in size was observed.

The loading of pilocarpine into the NPs has proved to be both a highly efficient and dynamic procedure, with really fast loadings within the first few minutes, and the NP–drug complexes were stable for months. It was observed that the higher the degree of cross-linking is, the higher is the amount of pilocarpine loaded into the NPs. Moreover, the Z-average and mean size of loaded NPs doubled and almost tripled in value for stabilized systems, giving weight to the observations mentioned above. Regarding the drug-release behavior, all of the systems experienced a boost in drug release at acidic pH, ranging from 50 to 80% within the first 48 h. NPs with 20% of core cross-linking delivered the highest percentage of drug at fixed times. Also significant were the release values from the non-cross-linked NPs, which may be due to some micellar disruption in the media.

The fine-tuned sustained release features encountered in the studied systems may provide a continuous delivery of the drug at specific acidic locations. Thereby, problems associated to cyclic variations in drug concentration in blood versus time may be averted, offering a maximum pharmacological efficiency at a minimum drug dose.

EXPERIMENTAL SECTION

The detailed procedures for the preparation of micelles by self-assembly, stabilization in the core, loading, and release assays, as well as all characterization techniques are available in the Supporting Information.

ASSOCIATED CONTENT

Supporting Information

The Supporting Information is available free of charge on the ACS Publications website at DOI: 10.1021/acsomega.7b01421.

Materials and methods (PDF)

AUTHOR INFORMATION

Corresponding Author

*E-mail: vdepaz@us.es.

ORCID

Elsa Galbis: 0000-0001-8521-2835

Nieves Iglesias: 0000-0003-0201-883X

M.-Violante de-Paz: 0000-0002-6544-4732

Juan A. Galbis: 0000-0001-8662-2852

Author Contributions

The manuscript was written through contributions of all authors. All authors have given approval to the final version of the manuscript.

Notes

The authors declare no competing financial interest.

ACKNOWLEDGMENTS

The authors would like to thank the Ministerio de Economía y Competitividad (Grant MAT2016-77345-C3-2-P) and the Junta de Andalucía (Grant P12-FQM-1553) of Spain for financial support.

REFERENCES

- (1) Karimi, M.; Ghasemi, A.; Zangabad, P. S.; Rahighi, R.; Moosavi Basri, S. M.; Mirshekari, H.; Amiri, M.; Shafaei Pishabad, Z.; Aslani, A.; Bozorgomid, M.; Ghosh, D.; Beyzavi, A.; Vaseghi, A.; Aref, A. R.; Haghani, L.; Bahrami, S.; Hamblin, M. R. Smart Micro/Nanoparticles in Stimulus-Responsive Drug/Gene Delivery Systems. *Chem. Soc. Rev.* **2016**, *45*, 1457.
- (2) Alvarez-Lorenzo, C.; Concheiro, A. Smart Drug Delivery Systems: From Fundamentals to the Clinic. *Chem. Commun.* **2014**, *50*, 7743–7765.
- (3) Wolinsky, J. B.; Colson, Y. L.; Grinstaff, M. W. Local Drug Delivery Strategies for Cancer Treatment: Gels, Nanoparticles, Polymeric Films, Rods, and Wafers. *J. Controlled Release* **2012**, *159*, 14–26.
- (4) Zhao, X.; Liu, P. Reduction-Responsive Core-Shell-Corona Micelles Based on Triblock Copolymers: Novel Synthetic Strategy, Characterization, and Application as a Tumor Microenvironment-Responsive Drug Delivery System. *ACS Appl. Mater. Interfaces* **2015**, *7*, 166–174.
- (5) Wang, Y.; Wang, J.; Wang, T.; Xu, Y.; Shi, L.; Wu, Y.; Li, L.; Guo, X. Pod-Like Supramicelles with Multicompartment Hydrophobic Cores Prepared by Self-Assembly of Modified Chitosan. *Nano-Micro Lett.* **2016**, *8*, 151–156.
- (6) Rheingans, O.; Hugenberg, N.; Harris, J. R.; Fischer, K.; Maskos, M. Nanoparticles Built of Cross-Linked Heterotelechelic, Amphiphilic Poly(dimethylsiloxane)-B-Poly(ethylene Oxide) Diblock Copolymers. *Macromolecules* **2000**, *33*, 4780–4790.
- (7) Galbis, E.; De-Paz, M.-V.; Iglesias, N.; Lucas, R.; Galbis, J. A. pH-Responsive Polymeric Nanoparticles as Drug Delivery Systems. *J. Drug Des. Res.* **2017**, *4*, 1047.
- (8) Garofalo, C.; Capuano, G.; Sottile, R.; Talerico, R.; Adami, R.; Reverchon, E.; Carbone, E.; Izzo, L.; Pappalardo, D. Different Insight into Amphiphilic PEG-PLA Copolymers: Influence of Macromolecular Architecture on the Micelle Formation and Cellular Uptake. *Biomacromolecules* **2014**, *15*, 403–415.
- (9) Li, Y.; Lokitz, B. S.; Armes, S. P.; McCormick, C. L. Synthesis of Reversible Shell Cross-Linked Micelles for Controlled Release of Bioactive Agents. *Macromolecules* **2006**, *39*, 2726–2728.
- (10) Dinu, I. A.; Duskey, J. T.; Car, A.; Palivan, C. G.; Meier, W. Engineered Non-Toxic Cationic Nanocarriers with Photo-Triggered Slow-Release Properties. *Polym. Chem.* **2016**, *7*, 3451–3464.
- (11) Salmaso, S.; Semenzato, A.; Bersani, S.; Matricardi, P.; Rossi, F.; Caliceti, P. Cyclodextrin/PEG Based Hydrogels for Multi-Drug Delivery. *Int. J. Pharm.* **2007**, *345*, 42–50.
- (12) Chang, Y.; Xiao, L. Preparation and Characterization of a Novel Drug Delivery System: Biodegradable Nanoparticles in Thermosensitive Chitosan/Gelatin Blend Hydrogels. *J. Macromol. Sci., Part A* **2010**, *47*, 608–615.
- (13) Biswas, S.; Kumari, P.; Lakhani, P. M.; Ghosh, B. Recent Advances in Polymeric Micelles for Anti-Cancer Drug Delivery. *Eur. J. Pharm. Sci.* **2016**, *83*, 184–202.
- (14) Liu, S.; Weaver, J. V. M.; Tang, Y.; Billingham, N. C.; Armes, S. P.; Tribe, K. Synthesis of Shell Cross-Linked Micelles with pH-Responsive Cores Using ABC Triblock Copolymers. *Macromolecules* **2002**, *35*, 6121–6131.
- (15) Galbis, E.; de-Paz, M.-V.; Iglesias, N.; Lacroix, B.; Alcudia, A.; Galbis, J. A. Core Cross-Linked Nanoparticles from Self-Assembling Polyfma-Based Micelles. Encapsulation of Lipophilic Molecules. *Eur. Polym. J.* **2017**, *89*, 406–418.
- (16) Mandal, B.; Bhattacharjee, H.; Mittal, N.; Sah, H.; Balabathula, P.; Thoma, L. A.; Wood, G. C. Core-Shell-Type Lipid-Polymer Hybrid Nanoparticles as a Drug Delivery Platform. *Nanomedicine* **2013**, *9*, 474–491.
- (17) de Paz Bãñez, M. V.; Robinson, K. L.; Butun, V.; Armes, S. P. Use of Oxyanion-Initiated Polymerization for the Synthesis of Amine Methacrylate-Based Homopolymers and Block Copolymers. *Polymer* **2001**, *42*, 29–37.
- (18) Mu, Q. S.; Lu, J. R.; Ma, Y. H.; de Paz Banez, M. V.; Robinson, K. L.; Armes, S. P.; Lewis, A. L.; Thomas, R. K. Neutron Reflection Study of a Water-Soluble Biocompatible Diblock Copolymer Adsorbed at the Air/Water Interface: The Effects of pH and Polymer Concentration. *Langmuir* **2006**, *22*, 6153–6160.
- (19) Bütün, V.; Wang, X.-S.; de Paz Banez, M. V.; Robinson, K. L.; Billingham, N. C.; Armes, S. P.; Tuzar, Z. Synthesis of Shell Cross-Linked Micelles at High Solids in Aqueous Media. *Macromolecules* **2000**, *33*, 1–3.
- (20) Galbis, E.; de Paz, M. V.; McGuinness, K. L.; Angulo, M.; Valencia, C.; Galbis, J. A. Tandem ATRP/Diels-Alder Synthesis of polyHEMA-Based Hydrogels. *Polym. Chem.* **2014**, *5*, 5391–5402.
- (21) Vivino, F. B.; Al-Hashimi, I.; Khan, Z.; et al. Pilocarpine Tablets for the Treatment of Dry Mouth and Dry Eye Symptoms in Patients With Sjogren Syndrome. *Arch. Intern. Med.* **1999**, *159*, 174–181.
- (22) Belström, D.; Holmstrup, P.; Fiehn, N. E.; Rosing, K.; Bardow, A.; Paster, B. J.; Pedersen, A. M. L. Bacterial Composition in Whole Saliva from Patients with Severe Hyposalivation - a Case-Control Study. *Oral Dis.* **2016**, *22*, 330–337.
- (23) Bardow, A.; Moe, D.; Nyvad, B.; Nauntofte, B. The Buffer Capacity and Buffer Systems of Human Whole Saliva Measured without Loss of CO₂. *Arch. Oral Biol.* **2000**, *45*, 1–12.
- (24) Zhang, L.; Su, T.; He, B.; Gu, Z. Self-Assembly Polyrotaxanes Nanoparticles as Carriers for Anticancer Drug Methotrexate Delivery. *Nano-Micro Lett.* **2014**, *6*, 108–115.
- (25) Kwon, G. S.; Naito, M.; Kataoka, K.; Yokoyama, M.; Sakurai, Y.; Okano, T. Block Copolymer Micelles as Vehicles for Hydrophobic Drugs. *Colloids Surf., B* **1994**, *2*, 429–434.